Postprint of: Czyżniewski M., Łangowski R., Piotrowski R., Respiration rate estimation using non-linear observers in application to wastewater treatment plant, JOURNAL OF PROCESS CONTROL Vol. 124 (2023), pp. 70-82, DOI: 10.1016/j.jprocont.2023.02.008

Respiration rate estimation using non-linear observers in application to wastewater treatment plant

Mateusz Czyżniewski[a], Rafał Łangowski[a,*] and Robert Piotrowski[a]

[a]*Department of Intelligent Control and Decision Support Systems, Gdańsk University of Technology, G. Narutowicza 11/12, Gdańsk, 80-233, Poland*

ARTICLE INFO

Keywords:
bioreactors
nonlinear observers
process modeling
respiration rate estimation
wastewater treatment plant

ABSTRACT

A problem of respiration rate estimation using two new non-linear observers for a wastewater treatment plant is addressed in this paper. In particular, a non-linear adaptive Luenberger-like observer and a super twisting sliding mode observer have been derived to produce stable and bounded estimates of the respiration rate. During the synthesis of the particular observer, an appropriate mathematical utility model was used. The observability analysis of this model was performed using a method of indistinguishable state trajectories. The stability of the devised observers was proved using the Lyapunov stability theory. The performance of the developed observers was validated by simulation using ranges of data from the case study wastewater treatment plant. Satisfactory results have been obtained and they demonstrate high effectiveness of the devised observers.

1. Introduction

Nowadays, efficient handling of most of the systems (plants) perceived as essential for the comfortable functioning of modern society requires advanced monitoring and control algorithms. These include systems such as power systems, transport systems, or environmental systems, e.g., drinking water distribution systems and biological wastewater treatment plants (WWTPs). To cope with the above, the mentioned algorithms should be equipped with instruments such as estimation, optimisation, diagnostics, etc. Moreover, the issue of access to the information on process variables is also involved. Typically, these variables include system state variables and controlled output variables (signals) of the system. Unfortunately, from operational practice, the access to these variables, especially state variables, is limited [6, 22]. It is therefore necessary to have an instrument to supply the missing information on state variables. Such a tool is a state observer (estimator) that generates estimates of unmeasured state variables, primarily. Typically, the reconstruction (estimation) of the system state is based on other available measured variables, so-called system measured outputs, and the mathematical model of a given plant. The topic undertaken in this paper concerns the reconstruction of state variables in WWTPs. In industrial practice, two main kinds of biological WWTPs are distinguished, i.e., on-flow WWTPs and sequencing batch reactors (SBRs) [32]. It should be noted that from the point of view of the nature of biological wastewater treatment, the processes taking place in both types of WWTPs are analogous. In the following part of the paper, an SBR-type wastewater treatment plant is considered. Biochemical processes in the WWTP are responsible for the elimination of contaminants that have not been removed during mechanical pre-treatment. These include in particular nitrification and denitrification for removal of nitrogen, and dephosphatation for removal of phosphorus [16, 17, 32]. These processes are carried out by micro-organisms called activated sludge or biomass. The requirement to achieve proper multiplication of the activated sludge is to provide it with an appropriate concentration of dissolved oxygen ($DO(t)$). To carry out biological reactions, it is therefore necessary to aerate the sewage. In other words, the denitrification, nitrification and dephosphatation processes are dependent on the concentration of $DO(t)$ in the WWTP.

The proper dissolved oxygen concentration is affected by two crucial process variables. The first one, denoted by $k_L a\left(Q_{\text{air}}(t)\right)$, is the function describing the transfer of oxygen into sewage through the aeration system and is often the control input in dissolved oxygen concentration control systems [32, 36, 48]. The second variable is respiration, denoted by $R(t)$ representing the oxygen consumption rate as a result of the oxygen uptake of micro-organisms and is often perceived as the disturbance input in dissolved oxygen concentration control systems [12, 18, 24, 36]. Both variables

*Corresponding author
rafal.langowski@pg.edu.pl (R. Łangowski)
ORCID(s): 0000-0003-3267-9006 (M. Czyżniewski); 0000-0003-1150-9753 (R. Łangowski); 0000-0002-8660-300X (R. Piotrowski)

are not only important for dissolved oxygen concentration control but also for process monitoring and diagnostics. It is because $k_{\mathrm{L}}a\left(Q_{\mathrm{air}}(t)\right)$ may be used for improving the performance of the control system, whereas $R(t)$ is a key indicator of current sewage load and biomass activity. Typically, direct on-line measurements of $k_{\mathrm{L}}a\left(Q_{\mathrm{air}}(t)\right)$ and $R(t)$ are not available in WWTPs. This is, among other, reasons due to a very high cost of respirometers capable of measuring respiration [27, 34, 42, 47]. These variables are, therefore estimated based on measurements of the airflow and dissolved oxygen concentration, and proper models of the processes. Different types of grey-box models, such as multiplicative-linear, multiplicative-affine, and exponential-non-linear model, are usually used for estimating $k_{\mathrm{L}}a\left(Q_{\mathrm{air}}(t)\right)$ [15, 24, 25]. In turn, the value of respiration or respiration rate is assessed using Kalman filters [4, 24, 25, 40, 41, 43], algorithms based on solving optimisation problems [26, 46], Luenberger-like observers [18], or high-gain observers [5]. Naturally, the aforementioned estimation algorithms have various features, e.g., the need to meet appropriate assumptions in Kalman filters, or a considerable computation time when solving optimisation tasks. Hence, this issue is still relevant in research work.

The main aim of this work is to provide two new respiration rate observers, i.e., the non-linear adaptive Luenberger-like observer (ALO) and the non-linear super twisting sliding mode observer (STSMO). A one-dimensional non-linear balance mathematical model for the aeration process in SBR from [20, 25, 36, 48] has been used as a cognitive model. Due to considering the respiration rate behaviour, the derived (utility) model for the synthesis of the developed observers is characterised by extending the original (cognitive) dynamics with an additional slowly time-varying state variable. The observability analysis of the utility model is also given. The performance of the developed observers was simulation-verified, using the ranges of data from the Swarzewo SBR WWTP [37]. To summarise, the main contributions of this paper are as follows:

a) a proper utility model for observer design purposes has been developed,

b) an observability analysis performed by applying a method of indistinguishable state trajectories has been given,

c) two new non-linear state observers producing stable and bounded (robust) estimates of the respiration rate have been derived, along with the discussion of the observers' gains selection methodology,

d) a comprehensive simulation analysis, including both scenarios noise free and noise affected, has been shown.

The paper is organised as follows. Section 2 includes the description of the cognitive model of dissolved oxygen concentration and the derivation of the utility model with an analysis of its observability. The synthesis of the non-linear adaptive Luenberger-like observer and the non-linear super twisting sliding mode observer for respiration rate estimation is given in Section 3. The obtained simulation results are discussed in Section 4. The paper is concluded in Section 5.

2. Modelling of dissolved oxygen concentration dynamics

A one-dimensional non-linear model of dissolved oxygen concentration dynamics is given as follows [20, 25, 36, 48]:

$$\dot{DO}(t) = -\frac{DO(t)}{K_{\mathrm{DO}}(t) + DO(t)} R(t) + k_{\mathrm{L}}a\left(Q_{\mathrm{air}}(t)\right)\left(DO_{\mathrm{sat}}\left(T(t)\right) - DO(t)\right), \tag{1}$$

where: $\dot{(\cdot)}$ stands for the derivative with respect to t; $t \in \mathbb{T} = \mathbb{R}_+ \cup \{0\}$ is the time instant, $\mathbb{R}_+$ denotes the positive part of $\mathbb{R}$; $DO(t)$ $\left[\mathrm{g\,O_2/m^3}\right] \in \mathbb{R}_+$ is the dissolved oxygen concentration; $R(t)$ $\left[\mathrm{g/m^3\,h}\right] \in \mathbb{R}_+$ signifies the respiration; $k_{\mathrm{L}}a\left(Q_{\mathrm{air}}(t)\right)$ $\left[1/\mathrm{h}\right] \in \mathbb{R}_+$ is the oxygen transfer function (continuous and differentiable with respect to $Q_{\mathrm{air}}(t)$) into sewage through the aeration system; $Q_{\mathrm{air}}(t)$ $\left[\mathrm{m^3/h}\right] \in \mathbb{R}_+$ denotes the airflow to tank (bioreactor); $DO_{\mathrm{sat}}\left(T(t)\right)$ $\left[\mathrm{g\,O_2/m^3}\right] \in \mathbb{R}_+$ stands for the dissolved oxygen saturation concentration; $T(t)$ $[^{\circ}C] \in \mathbb{R}_+$ denotes the temperature of sewage in the bioreactor; $K_{\mathrm{DO}}(t)$ $\left[\mathrm{g\,O_2/m^3}\right] \in \mathbb{R}_+$ is the unknown saturation parameter of the dissolved oxygen concentration dynamics.

It is worth adding that the first product on the right-hand side of (1) is often called the respiration rate and is designated as $\tilde{R}(t)$ $\left[\mathrm{g/m^3\,h}\right] \in \mathbb{R}_+$ [15, 18, 25, 40]. Moreover, by their nature, in the operational conditions when $Q_{\mathrm{air}}(t)$ is non-zero (aerobic phase), all variables in model (1) are positive and bounded, i.e.:

$$0 < \underline{DO} \leq DO(t) \leq \overline{DO},\ 0 < \underline{R} \leq R(t) \leq \overline{R},\ 0 < \underline{k_{\mathrm{L}}a} \leq k_{\mathrm{L}}a\left(Q_{\mathrm{air}}(t)\right) \leq \overline{k_{\mathrm{L}}a},$$

$$0 < \underline{Q_{\mathrm{air}}} \leq Q_{\mathrm{air}}(t) \leq \overline{Q_{\mathrm{air}}},\ 0 < \underline{T} \leq T(t) \leq \overline{T},\ 0 < \underline{K_{\mathrm{DO}}} \leq K_{\mathrm{DO}}(t) \leq \overline{K_{\mathrm{DO}}},$$

where $\underline{(\cdot)}$ and $\overline{(\cdot)}$ are the real and positive upper and lower bounds on the particular variable.

As it has been mentioned, respiration represents the oxygen consumption rate being the result of the oxygen uptake of micro-organisms. This phenomenon depends on many factors that can be divided into three main groups: biomass source, type of substrate, and temporal aspect [25]. Theoretically, respiration can be determined from the extended models, e.g., ASM2d where exact non-linear kinetics functions (growth rates) express complex relations between biochemical compounds residing in the bioreactor [16]. On the other hand, respiration can be measured using specialised measuring devices called respirometers [27, 34, 42, 47]. However, due to the mentioned complexity of the ASM family models, as well as the high cost of respirometers, these possibilities are considerably limited. Hence, there arises an interest in using respiration estimation algorithms.

Remark 1. The oxygen concentration is delivered to WWTP by the aeration system. This system is composed of blowers, pipes and diffusers. Since the dynamics of this system is much faster than the dynamics of biochemical processes, as well as, there are no variables directly involved in model (1), it can be modelled as a static system with a gain of one for estimation purposes.

Assumption 1. *The oxygen transfer function $k_{\mathrm{L}}a\left(Q_{\mathrm{air}}(t)\right)$ is a linearly $Q_{\mathrm{air}}(t)$-dependent input to the model for observer synthesis (utility model).*

The oxygen transfer function is mainly influenced by airflow, atmospheric pressure, and the type of diffusers deriving air to the bioreactor and their depth of immersion. However, the airflow is the crucial factor [24, 36]. When analysing the properties of the model of dissolved oxygen dynamics, the most often used $k_{\mathrm{L}}a\left(Q_{\mathrm{air}}(t)\right)$ models are the linear, exponential, and cubic spline models [24]. Knowing the value of $Q_{\mathrm{air}}(t)$, it is assumed that $k_{\mathrm{L}}a\left(Q_{\mathrm{air}}(t)\right)$ is a linearly $Q_{\mathrm{air}}(t)$-dependent input to the utility model, i.e. $k_{\mathrm{L}}a\left(Q_{\mathrm{air}}(t)\right) \triangleq \alpha Q_{\mathrm{air}}(t)$, where $\alpha \in \mathbb{R}_{+}$ is the scaling parameter.

Assumption 2. *The dissolved oxygen saturation concentration $DO_{\mathrm{sat}}(T(t))$ is a $T(t)$-dependent input to the model for observers synthesis.*

In fact, $DO_{\mathrm{sat}}(T(t))$ can be considered as the time-varying variable, the time-variation of which is dependent on factors such as: sewage composition, atmospheric pressure, tank geometry, and air humidity and primarily temperature [3, 24, 32]. Therefore, to obtain the value of $DO_{\mathrm{sat}}(T(t))$, it is assumed that the temperature at a given pressure is the main influencing factor.

2.1. Model of dissolved oxygen concentration for observer synthesis

To perform the observer synthesis, the model of dissolved oxygen concentration dynamics (1) must be revised for use as the utility model. Firstly, it is due to the properties of the respiration $R(t)$. This variable is slowly time-varying. Thus, according to the methodology from [10, 45], $R(t)$ may be treated as an additional dynamic variable. This proposition has been introduced in the literature for not only reconstruction of $R(t)$ separately but also for the estimation of the respiration rate $\tilde{R}(t)$ [4, 15, 40]. Moreover, the value of $K_{\mathrm{DO}}(t)$ is typically unknown and consequently, the reconstruction of $R(t)$ becomes very challenging. Therefore, a typical approach is to estimate the respiration rate $\tilde{R}(t)$ rather than the respiration itself. Secondly, the resolution of input issues must be premised on appropriate regarding of properties of $k_{\mathrm{L}}a\left(Q_{\mathrm{air}}(t)\right)$ and $DO_{\mathrm{sat}}(T(t))$. According to Assumption 1, the oxygen transfer function can be treated as a direct input to the utility model. In the context of the second variable, knowing that the temperature of sewage can be easily and precisely measured and the characteristic between the temperature and dissolved oxygen saturation concentration is known, $DO_{\mathrm{sat}}(T(t))$ can be treated as an additional input to the utility model (see Assumption 2).

To perform the observer synthesis, the first state variable is simply defined as:

$$x_1(t) \triangleq DO(t). \tag{2}$$

Next, an auxiliary variable $P(t) \in \mathbb{R}_{-}\ [-]$, where $\mathbb{R}_{-}$ denotes the negative part of $\mathbb{R}$, which consists of the combination of the negative value of $R(t)$ and $\left[K_{\mathrm{DO}}(t) + DO(t)\right]^{-1}$ is introduced. It is chosen to cancel the impact

of $K_{\mathrm{DO}}(t)$ on the considered dynamics and to simplify the process of $\tilde{R}(t)$ reconstruction. Hence, the second state variable and $\tilde{R}(t)$ yields:

$$\begin{aligned} x_2(t) &\triangleq P(t) = -R(t)\left[K_{\mathrm{DO}}(t) + DO(t)\right]^{-1}, \\ \tilde{R}(t) &\triangleq -x_1(t)x_2(t). \end{aligned} \tag{3}$$

Taking into account that the second state variable $x_2(t)$ has been introduced, model (1) must be extended by a new dynamical term. By invoking the literature presenting the methods devised for the estimation of unknown kinetics functions of other biochemical processes, e.g., [8, 9, 31, 35], the $P(t)$ related differential equation can be proposed by using dissolved oxygen concentration proportional representation given as:

$$\dot{P}(t) \triangleq r(t)x_1(t), \tag{4}$$

where $r(t) \in \mathbb{R}$ is the time-varying function representing an uncertainty in system dynamics.

The explicit form of $r(t)$ can be established by the appropriate combination of highly non-linear derivatives of specific kinetics function terms such as Monod, Haldane, etc. components, which constitute the functional form of $R(t)$ (part of $P(t)$ introduced in (3)) [16, 24, 48]. Despite that, due to the inherent complexity of kinetics functions, the estimation methodology presented in the paper does not rely on knowing the direct form of $r(t)$ but is premised on considering it as the uniformly bounded unknown input.

Taking $k_{\mathrm{L}}a\left(Q_{\mathrm{air}}(t)\right)$ as an exogenous signal, as discussed earlier, the first input is given as:

$$u_1(t) \triangleq k_{\mathrm{L}}a\left(Q_{\mathrm{air}}(t)\right). \tag{5}$$

In turn, the second input is derived from the linear multiplication of $k_{\mathrm{L}}a\left(Q_{\mathrm{air}}(t)\right)$ and $DO_{\mathrm{sat}}\left(T(t)\right)$:

$$u_2(t) \triangleq k_{\mathrm{L}}a\left(Q_{\mathrm{air}}(t)\right) DO_{\mathrm{sat}}\left(T(t)\right). \tag{6}$$

Hence, by combining model (1) with (2) - (6), the following non-linear state-space utility model Σ_{U} is obtained:

$$\Sigma_{\mathrm{U}}: \begin{cases} \dot{x}_1(t) &= x_1(t)x_2(t) - u_1(t)x_1(t) + u_2(t) \\ \dot{x}_2(t) &= r(t)x_1(t) \\ \tilde{R}(t) &= -x_1(t)x_2(t) \\ y(t) &= x_1(t) \\ \boldsymbol{x}(t_0) &= \boldsymbol{x}_0 \end{cases}, \tag{7}$$

where $\boldsymbol{x}_0 \in \mathbb{R}^2_+$ denotes the vector of initial conditions.

Moreover, the following assumptions are made:

Assumption 3. *The state variable $x_1(t)$ is measurable, with its measurements burdened by measurement noise modelled as white Gaussian noise.*

Assumption 4. *The unknown time-varying function $r(t)$ is uniformly bounded, i.e., $\forall t \in \mathbb{T}\ |r(t)| \leq \overline{r} \in \mathbb{R}_+$. Also, due to boundedness of $DO(t)$, the derivative of the respiration rate is bounded uniformly: $\forall t \in \mathbb{T}\ \left|\dot{\tilde{R}}(t)\right| \leq \overline{r}\,\overline{DO}$.*

Assumption 5. *Both known inputs are the permanently excited positive signals due to the physical properties of the considered system, i.e. [21]:*

$$\underline{\alpha}_{\mathrm{u}}\boldsymbol{I}_{2\times 2} \leq \int_t^{T_{\mathrm{p}}+t} \boldsymbol{u}(\tau)\boldsymbol{u}^{\mathrm{T}}(\tau)d\tau \leq \overline{\alpha}_{\mathrm{u}}\boldsymbol{I}_{2\times 2}, \tag{8}$$

where: $\underline{\alpha}_{\mathrm{u}} \in \mathbb{R}_+$, $\overline{\alpha}_{\mathrm{u}} \in \mathbb{R}_+$ are the lower and upper bounds of the permanently excited inputs; $T_{\mathrm{p}} \in \mathbb{T}$ is the selected time period; $\boldsymbol{I}_{2\times 2}$ is the identity matrix.

2.2. Observability analysis

To perform the observer synthesis, it is necessary to verify that the model of the considered system is observable. As can be noticed, model (7) is dependent on known and unknown inputs (exogenous signals). Hence, a method of indistinguishable state trajectories (indistinguishable dynamics) can be used to prove the observability of this model [7, 28, 30, 38]. In general, this approach is based on direct interpretation and utilisation of state trajectory indistinguishability definitions, where the natural extensions of the classical observability/detectability concepts are premised on the possibility of unique or asymptotic reconstruction of both state and unknown input trajectories. Hence, strong u-observability and strong u-detectability notions defined in [30] are directly incorporated into this research.

Briefly, the practical utilisation of this method is given as follows. For the assumed two structurally identical dynamical systems Σ_{U}, i.e., 'original' ($\boldsymbol{x}(t)$ dependent) system and 'copied' ($\boldsymbol{z}(t)$ dependent) system, the initial conditions of which are not equal, i.e., $\boldsymbol{x}_0 \neq \boldsymbol{z}_0$, it is checked how integral curve trajectories of states of the both systems evolve under the revealed identical input-output behaviour. In other words, whether $\forall t \in \mathbb{T}\ \lim_{t\to\infty} \|\boldsymbol{x}(t) - \boldsymbol{z}(t)\| \neq 0$ states are not detectable, $\lim_{t\to\infty} \|\boldsymbol{x}(t) - \boldsymbol{z}(t)\| = 0$ states are detectable, or $\boldsymbol{x}(t) \equiv \boldsymbol{z}(t)$ states are observable [7, 28, 30, 38]. The investigation is based on the analysis of the dynamic properties of the error, defined as follows:

$$\boldsymbol{\varepsilon}(t) \triangleq \boldsymbol{x}(t) - \boldsymbol{z}(t), \tag{9}$$

where $\boldsymbol{\varepsilon}(t) \in \mathbb{R}^2$ is the error between indistinguishable state trajectories.

However, due to the presence of the unknown time-varying function $r(t)$ and the respiration rate $\tilde{R}(t)$ in model (7) it is necessary to define the following additional error components:

$$\varepsilon_{\mathrm{r}}(t) \triangleq r(t) - r^*(t),\ \varepsilon_{\tilde{\mathrm{R}}}(t) \triangleq \tilde{R}(t) - \tilde{R}^*(t), \tag{10}$$

where $\varepsilon_{\mathrm{r}}(t) \in \mathbb{R}$ is the error between 'original' $r(t)$ and 'copied' $r^*(t) \in \mathbb{R}$ unknown input, and $\varepsilon_{\tilde{\mathrm{R}}}(t) \in \mathbb{R}$ denotes the error between 'original' $\tilde{R}(t)$ and 'copied' $\tilde{R}^*(t) \in \mathbb{R}_+$ respiration rate.

Hence, combining the dynamics Σ_{U} and the differentiated errors defined in (9) and (10) the following error dynamics Σ_{I} is obtained:

$$\Sigma_{\mathrm{I}}: \begin{cases} \dot{\varepsilon}_1(t) & = x_1(t)x_2(t) - u_1(t)\varepsilon_1(t) - \big(x_1(t) - \varepsilon_1(t)\big)\big(x_2(t) - \varepsilon_2(t)\big) \\ \dot{\varepsilon}_2(t) & = r(t)x_1(t) - \big(x_1(t) - \varepsilon_1(t)\big)\big(r(t) - \varepsilon_{\mathrm{r}}(t)\big) \\ \varepsilon_{\tilde{\mathrm{R}}}(t) & = -x_1(t)x_2(t) + \big(x_1(t) - \varepsilon_1(t)\big)\big(x_2(t) - \varepsilon_2(t)\big) \\ \varepsilon_1(t) & = 0 \\ \boldsymbol{\varepsilon}(t_0) & = \boldsymbol{\varepsilon}_0 \end{cases}. \tag{11}$$

By studying the properties of the error dynamics Σ_{I}, the observability/detectability of the system Σ_{U} may be proved. Firstly, (11) is transformed into a simplified version under Assumption 3, which causes that $\varepsilon_1(t)$ and $\dot{\varepsilon}_1(t)$ are equal to zero $\forall t \in \mathbb{T}$. Therefore, (11) yields:

$$\Sigma_{\mathrm{I}}: \begin{cases} 0 & = x_1(t)\varepsilon_2(t) \\ \dot{\varepsilon}_2(t) & = x_1(t)\varepsilon_{\mathrm{r}}(t) \\ \varepsilon_{\tilde{\mathrm{R}}}(t) & = -x_1(t)\varepsilon_2(t) \\ \boldsymbol{\varepsilon}(t_0) & = \boldsymbol{\varepsilon}_0 \end{cases}. \tag{12}$$

Secondly, the interpretation of properties of (12) is as follows. Knowing that the dissolved oxygen concentration is positive $\forall t \in \mathbb{T}$ (aerobic phase), $\varepsilon_2(t)$ and $\dot{\varepsilon}_2(t)$ must be always equal to zero. It implies that $x_2(t)$ is strongly u-observable. Moreover, it is easy to check that $\varepsilon_{\mathrm{r}}(t)$ and $\varepsilon_{\tilde{\mathrm{R}}}(t)$ must be equal to zero $\forall t \in \mathbb{T}$ due to $x_2(t)$ observability. Hence, the unknown time-varying function $r(t)$ is observable, and the respiration rate $\tilde{R}(t)$ can be exactly reconstructed.

3. Synthesis of observers for respiration rate estimation in WWTP

This section presents, the synthesis of the non-linear adaptive Luenberger-like observer (ALO) and the non-linear super twisting sliding mode observer (STSMO) for respiration rate estimation in WWTP.

3.1. Synthesis of ALO

The non-linear adaptive Luenberger-like observer is the development of the observer introduced in [2, 3, 11, 33]. The developed ALO enables to reconstruct of the respiration rate instead of estimating an unknown kinetics function by utilising the adaptive-proportional structure of the correction term. Taking into account form (7) of the utility model, the explicit formula of the right-hand side of $\dot{\tilde{R}}(t)$ is generally dedicated to avoid issues around the stability (boundedness) analysis and to simplify the selection of values of observer gains encountered in [2, 3, 11, 33]. The main difference between them and the here developed one is that the derivative of $\tilde{R}(t)$ is not only bounded by some constant parameter but also related to the dissolved oxygen proportional term introduced in model (7).

Theorem 1. Assume that the triple $\left(x_1(t), x_2(t), \tilde{R}(t)\right)$ represents the solution of system (7) $\forall t \in \mathbb{T}$. Then the following non-linear adaptive Luenberger-like observer:

$$\mathcal{O}_{\text{ALO}}: \begin{cases} \dot{\hat{x}}_1(t) &= \left[\hat{x}_2(t) - u_1(t) + K_1 e_1(t)\right] x_1(t) + u_2(t) \\ \dot{\hat{x}}_2(t) &= K_2 e_1(t) x_1(t) \\ \hat{\tilde{R}}(t) &= -x_1(t)\hat{x}_2(t) \\ \hat{\boldsymbol{x}}(t_0) &= \hat{\boldsymbol{x}}_0 \end{cases}, \tag{13}$$

guarantees the globally uniformly bounded estimates $\hat{x}_1(t)$, $\hat{x}_2(t)$ and $\hat{\tilde{R}}(t)$ of state variables $x_1(t)$, $x_2(t)$ and the respiration rate $\tilde{R}(t)$, respectively, with the robustness to $r(t)$ for properly selected values of the observer gains matrix $\boldsymbol{K} = \begin{bmatrix} K_1 & K_2 \end{bmatrix}^{\mathrm{T}} \in \mathbb{R}^2_+$.

The developed ALO (13) adopts the correction term to compensate the impact of unknown input $r(t)$. To select the values of the ALO gains matrix, the following approach based on second-order system pole placement methodology [3, 13, 33] is proposed: $K_1 = 2\zeta\omega$ and $K_2 = \omega^2$, where $\zeta \in \mathbb{R}_+$ is the damping rate and $\omega \in \mathbb{R}_+$ is the oscillation frequency.

Proof. By combining Σ_{U} and $\mathcal{O}_{\text{ALO}}$ the following estimation error dynamics is given:

$$\begin{cases} \dot{e}_1(t) &= \left[e_2(t) - K_1 e_1(t)\right] x_1(t) \\ \dot{e}_2(t) &= \left[r(t) - K_2 e_1(t)\right] x_1(t) \\ e_{\tilde{\text{R}}}(t) &= -x_1(t) e_2(t) \\ \boldsymbol{e}(t_0) &= \boldsymbol{e}_0 \end{cases} \equiv \begin{cases} \dot{\boldsymbol{e}}(t) &= \left[\boldsymbol{A}\boldsymbol{e}(t) + \boldsymbol{B}(t)\right] x_1(t) \\ e_{\tilde{\text{R}}}(t) &= -x_1(t) e_2(t) \\ \boldsymbol{e}(t_0) &= \boldsymbol{e}_0 \end{cases}, \tag{14}$$

where: $e_1(t) \triangleq x_1(t) - \hat{x}_1(t)$, $e_2(t) \triangleq x_2(t) - \hat{x}_2(t)$, $e_{\tilde{\text{R}}}(t) \triangleq \tilde{R}(t) - \hat{\tilde{R}}(t)$ are the estimation errors for the first and second state variables and the respiration rate, respectively, and matrix $\boldsymbol{A} \in \mathbb{R}^{2\times 2}$ and vector $\boldsymbol{B}(t) \in \mathbb{R}^2$ are given as:

$$\boldsymbol{A} = \begin{bmatrix} -K_1 & 1 \\ -K_2 & 0 \end{bmatrix}, \ \boldsymbol{B}(t) = \begin{bmatrix} 0 \\ r(t) \end{bmatrix}. \tag{15}$$

The quadratic Lyapunov function $\mathcal{V}(\boldsymbol{e}(t))$ yields [21, 29]:

$$\begin{aligned} &\mathcal{V}(\boldsymbol{e}(t)) = \boldsymbol{e}^{\mathrm{T}}(t)\boldsymbol{\mathcal{P}}\boldsymbol{e}(t), \\ &\lambda_{\min}(\boldsymbol{\mathcal{P}}) \|\boldsymbol{e}(t)\|^2 \leq \mathcal{V}(\boldsymbol{e}(t)) \leq \lambda_{\max}(\boldsymbol{\mathcal{P}}) \|\boldsymbol{e}(t)\|^2, \end{aligned} \tag{16}$$

where: $\boldsymbol{\mathcal{P}} \in \mathbb{R}^{2\times 2}$ is the real symmetric matrix; $\lambda_{\max}(\boldsymbol{\mathcal{P}}) \in \mathbb{R}$, $\lambda_{\min}(\boldsymbol{\mathcal{P}}) \in \mathbb{R}$ denote the largest and the smallest eigenvalues of $\boldsymbol{\mathcal{P}}$, respectively; $\|\cdot\|$ signifies a Euclidean norm of $(\cdot)$. Also, it is assumed that the estimation error

vector belongs to the convex and bounded domain, i.e., $\boldsymbol{e}(t) \in \mathcal{E} \subset \mathbb{R}^2 \ \forall t \in \mathbb{T}$, and the convex set $\overline{\boldsymbol{S}} = \left\{ \|\boldsymbol{e}(t)\| \leq \overline{\kappa} \mid \boldsymbol{e}(t) \in \boldsymbol{\mathcal{E}} \right\}$ for $\overline{\kappa} \in \mathbb{R}_+$ is given.

The time derivative of $\mathcal{V}(\boldsymbol{e}(t))$ yields:

$$\begin{aligned} \dot{\mathcal{V}}(\boldsymbol{e}(t)) &= \dot{\boldsymbol{e}}^{\mathrm{T}}(t)\boldsymbol{\mathcal{P}}\boldsymbol{e}(t) + \boldsymbol{e}^{\mathrm{T}}(t)\boldsymbol{\mathcal{P}}\dot{\boldsymbol{e}}(t) = \left(\boldsymbol{e}^{\mathrm{T}}(t)\left[\boldsymbol{A}^{\mathrm{T}}\boldsymbol{\mathcal{P}} + \boldsymbol{\mathcal{P}}\boldsymbol{A}\right]\boldsymbol{e}(t) + 2\boldsymbol{B}^{\mathrm{T}}(t)\boldsymbol{\mathcal{P}}\boldsymbol{e}(t)\right) x_1(t) \\ &= -\left(\boldsymbol{e}^{\mathrm{T}}(t)\boldsymbol{I}_{2\times 2}\boldsymbol{e}(t) - 2\boldsymbol{B}^{\mathrm{T}}(t)\boldsymbol{\mathcal{P}}\boldsymbol{e}(t)\right) x_1(t) < 0, \end{aligned} \tag{17}$$

where $-\boldsymbol{I}_{2\times 2} = \boldsymbol{A}^{\mathrm{T}}\boldsymbol{\mathcal{P}} + \boldsymbol{\mathcal{P}}\boldsymbol{A}$ signifies the Lyapunov equation [21].

Assuming that the vector $\boldsymbol{B}$ can be uniformly bounded, i.e., $\|\boldsymbol{B}(t)\| \leq \overline{r}$, the Lyapunov function derivative (17) can be assessed by the following expression:

$$\begin{aligned} \dot{\mathcal{V}}(\boldsymbol{e}(t)) &\leq -\left(\|\boldsymbol{e}(t)\|^2 - 2\lambda_{\max}(\boldsymbol{\mathcal{P}})\|\boldsymbol{B}(t)\|\,\|\boldsymbol{e}(t)\|\right) x_1(t) \leq -\left(\|\boldsymbol{e}(t)\| - 2\overline{r}\lambda_{\max}(\boldsymbol{\mathcal{P}})\right)\|\boldsymbol{e}(t)\|\, x_1(t) \\ &= -(1-\theta)\|\boldsymbol{e}(t)\|^2 x_1(t) + \left(2\overline{r}\lambda_{\max}(\boldsymbol{\mathcal{P}}) - \theta\|\boldsymbol{e}(t)\|\right)\|\boldsymbol{e}(t)\|\, x_1(t), \end{aligned} \tag{18}$$

for any parameter $\theta \in (0\ ;\ 1)$.

Thus, the global uniform boundedness can be guaranteed if the following condition is met:

$$\|\boldsymbol{e}(t)\| \geq 2\theta^{-1}\overline{r}\lambda_{\max}(\mathcal{P}) = \underline{\kappa} \in \mathbb{R}_+ \ \forall \boldsymbol{e}(t) \in \boldsymbol{\mathcal{E}}$$

Moreover, the ultimate bound $\xi \in \mathbb{R}_+$ can be calculated as [21]:

$$\xi = \sqrt{\lambda_{\max}(\mathcal{P})\,\lambda_{\min}^{-1}(\mathcal{P})}\underline{\kappa}.$$

In turn, the steady state respiration rate error $e_{\tilde{\mathrm{R}}}(t)$ is bounded in the following way: $\left|\left(e_{\tilde{\mathrm{R}}}(t)\right)\right| \leq e_2^*\overline{DO}$, where $e_2^* = \max\left\{\left|\left(\underline{e}_2\right)\right|,\ \left|\left(\overline{e}_2\right)\right|\right\}$ is the minimal absolute value of the second estimation error.

Thus, the state estimation error and the respiration rate estimation error are globally uniformly bounded despite unknown input $r(t)$.

□

Proof 3.1 validates the global and uniform boundedness of the estimation error using classical Lyapunov tools. In fact, this property is weaker than the global asymptotic stability. However, taking into account that the size of set $\underline{\boldsymbol{S}} = \left\{ \|\boldsymbol{e}(t)\| \geq \underline{\kappa} \mid \boldsymbol{e}(t) \in \boldsymbol{\mathcal{E}} \right\}$ is dependent on the value of $\overline{r}\lambda_{\max}(\boldsymbol{\mathcal{P}})$, the minimisation of $\underline{\kappa}$ can be guaranteed by appropriate selection of observer gains. Whereas the vector $\boldsymbol{K}$ can be adjusted during synthesis, the selection of $\overline{r}$ must be premised on a realistic consideration of respiration rate time variation.

Remark 2. According to [6], for particular form of matrix $\boldsymbol{A}$ from (15), the selection of $\boldsymbol{K}$ values certainly affects $\lambda_{\max}(\boldsymbol{\mathcal{P}})$, which results from the form of the Lyapunov function derivative (17). If the values of both observer gains are increasing, then $\lambda_{\max}(\boldsymbol{\mathcal{P}})$ becomes smaller. Whereas, when one of the observer gains is significantly bigger than the other, then $\lambda_{\max}(\boldsymbol{\mathcal{P}})$ is increasing. Hence, knowing that K_1 is dependent on the values of ζ and ω, as well as that K_2 is related only to ω, the pole placement must be related to selecting ζ close to 1 and $\omega >> 1$. It is due to avoiding too-long transient states (for significantly high damping rate values) and the over-activity of the correction term (unnecessary oscillations). This is the consequence of insisting on making $\lambda_{\max}(\boldsymbol{\mathcal{P}})$ as small as possible to ensure feasibility at the most minimal value of $\underline{\kappa}$ and to guarantee satisfying dynamical properties of the observer.

3.2. Synthesis of STSMO

The developed non-linear super twisting sliding mode observer is based on the algorithm introduced in [8, 9], where the problem of uncertain kinetics function reconstruction has been addressed for a given class of biochemical processes. In the context of application issues, super twisting algorithms reveal interesting and desirable properties [14, 23, 29]. These include the finite time of convergence $T_{\mathrm{STSMO}} \in \mathbb{T}$ (global uniform asymptotic stability [21]), high robustness with respect to selected uncertainty $r(t)$, and very high accuracy of the reconstruction process when the measurement is noise-free, i.e.: $\hat{r}(t) \equiv r(t)\ \forall t > T_{\mathrm{STSMO}}$. Nevertheless, those methods are very sensitive to the factors such as measurement errors and noise and other uncertainties occurring in a given system model.

In order to use the methodology outlined in [8, 9], the utility model (7) must be extended accordingly. More specifically, the model must have such a form that its solution satisfies the differential inclusion, i.e., the solution in the sense of Filipov [44]. Therefore, model (7) is transformed to the following form:

$$\mathcal{P}_{\mathrm{U}}: \begin{cases} \dot{x}_1(t) & = \left[x_2(t) - u_1(t)\right] x_1(t) + u_2(t) \\ \dot{x}_2(t) & \in U\bar{r}x_1(t) \\ \tilde{R}(t) & = -x_1(t)x_2(t) \\ y(t) & = x_1(t) \\ \boldsymbol{x}(t_0) & = \boldsymbol{x}_0 \end{cases}, \tag{19}$$

where $U = [-1\ ;\ +1] \in \mathbb{R}$ is the convex set. The differential inclusion of (19) represents all of the state solutions satisfying Assumption 4.

Theorem 2. Assume that the triple $\left(x_1(t), x_2(t), \tilde{R}(t)\right)$ represents the solution in the sense of Filipov of system (19) $\forall t \in \mathbb{T}$. Then the following non-linear super twisting sliding mode observer:

$$\mathcal{O}_{\mathrm{STSMO}}: \begin{cases} \dot{\hat{x}}_1(t) & = \left[\hat{x}_2(t) - u_1(t) + 2\beta_1\sqrt{\bar{r}\left|e_1(t)\right|}\mathrm{sgn}\left(e_1(t)\right)\right] x_1(t) + u_2(t) \\ \dot{\hat{x}}_2(t) & = \beta_2\mathrm{sgn}\left(e_1(t)\right)\bar{r}x_1(t) \\ \hat{\tilde{R}}(t) & = -x_1(t)\hat{x}_2(t) \\ \hat{\boldsymbol{x}}(t_0) & = \hat{\boldsymbol{x}}_0 \end{cases} \tag{20}$$

guarantees the global uniform asymptotic stability of the estimation error in time $T_{\mathrm{STSMO}} \in \mathbb{T}$ related to the robustness with respect to $r(t)$ for properly selected values of $\bar{r}$ and tuning parameters $\beta_1 \in \mathbb{R}_+$ and $\beta_2 \in (1\ ;\ \infty)$.

The uniform convergence of the observer (20) may be proved by using standard Lyapunov tools adjusted to the properties of the sliding mode regimes [9, 29]. The analysis is performed in two ways by applying the direct Lyapunov method for quadratic stability investigation. Firstly, assuming that the tuning parameters are properly selected, the global uniform asymptotic stability is justified. Secondly, by using polytopic differential inclusions and linear matrix inequality tools, the conditions for selecting β_1 and β_2 are given.

Proof. By combining $\mathcal{P}_{\mathrm{U}}$ and $\mathcal{O}_{\mathrm{STSMO}}$ the following estimation error dynamics is given:

$$\begin{cases} \dot{e}_1(t) & = \left[e_2(t) + 2\beta_1\sqrt{\bar{r}\left|e_1(t)\right|}\mathrm{sgn}\left(e_1(t)\right)\right] x_1(t) \\ \dot{e}_2(t) & \in \left[U - \beta_2\mathrm{sgn}\left(e_1(t)\right)\right]\bar{r}x_1(t) \\ e_{\tilde{\mathrm{R}}}(t) & = -x_1(t)e_2(t) \\ \boldsymbol{e}(t_0) & = \boldsymbol{e}_0 \end{cases}, \tag{21}$$

Due to the fact that the estimation error dynamics (21) ideally fits into equation (15) from [9], the stability considerations are only narrowed to show that $\tilde{R}(t)$ can be estimated by (20). This can be deduced from the third equation of (21) in which an algebraic term occurs. Taking into account that $x_1(t)$ is the measured positive variable and $e_2(t)$ converges to zero in finite time for any initial conditions, $e_{\tilde{\mathrm{R}}}(t)$ must tend to zero in the same way as $\boldsymbol{e}(t)$. Therefore, the respiration rate $\tilde{R}(t)$ can be uniformly and asymptotically reconstructed in time T_{STSMO} for any initial conditions.

□

Remark 3. The selection of β_1 and β_2 is conditioned by the Lyapunov stability analysis [9]. In turn, for selected higher values of $\bar{r}$, the convergence rate is more rapid and the robustness against the impact of $r(t)$ increases. However, the reconstruction performance becomes more susceptible to the influence of errors and measurement noise.

Moreover, due to fact that the functions sgn(·) and |(·)| are discontinuous, their smooth approximations are proposed to avoid the chattering phenomenon [23, 44]. For the sgn(·) approximation, the $\chi(\cdot)$ function yields:

$$\operatorname{sgn}(\cdot) \simeq \chi(\cdot) = \frac{(\cdot)}{\gamma + |(\cdot)|}, \tag{22}$$

where $\gamma \in \mathbb{R}_+$ denotes the tuning parameter.

In turn, for |(·)| function, the regularisation approach is proposed which consists in introducing the continuous function $\psi(\cdot)$ [39] given by:

$$|(\cdot)| \simeq \psi(\cdot) = c^{-1}\left[\log\left(1+\exp(c(\cdot))\right) + \log\left(1+\exp(-c(\cdot))\right)\right], \tag{23}$$

where $c \in \mathbb{R}_+$ is the tuning parameter.

Remark 4. It is worth adding that even when the estimation error converges to the small sphere (close neighborhood of the sliding surface $e_1(t) = 0$) during the appearance of measurement noise or when the measurement process is corrupted by inertial dynamics of the measuring device, the uniform stability is still guaranteed even when the observer becomes more sensitive and reactive. To partially suppress the negative impact related to measurement quality, the parameters of functions $\chi(\cdot)$ and $\psi(\cdot)$ can be adjusted.

4. Case study

The devised observers (13) and (20) have been applied to the non-linear model of dissolved oxygen concentration dynamics (1). This model and all observers were implemented in the Matlab/Simulink environment.

The values of the particular parameters and variables were established as follows. According to Assumption 2, the values of dissolved oxygen saturation concentration $DO_{\text{sat}}(T(t))$ were assumed known and time-varying. They result from [24]:

$$DO_{\text{sat}}(T(t)) = \beta_{\text{sat}}\, DO_{\text{sat}}^{\text{water}}(T(t)),$$

where $\beta_{\text{sat}} \in \mathbb{R}_+$ is the constant parameter experimentally determined for a given WWTP, and $DO_{\text{sat}}^{\text{water}}(T(t)) \in \mathbb{R}_+$ is the dissolved oxygen saturation concentration for (clean) water. The values of $DO_{\text{sat}}^{\text{water}}(T(t))$ over a wide temperature range at a given atmospheric pressure can be found in the literature, e.g., [1]. Therefore, in this study, using the values of $DO_{\text{sat}}(T(t))$ determined for particular temperature measurements available in the literature and comparing them with the corresponding water-related equivalents, the value of β_{sat} was assumed as $\beta_{\text{sat}} = 0.98$ [−]. Then, for known values of $DO_{\text{sat}}^{\text{water}}(T(t))$ and assuming the typical value of atmospheric pressure, i.e., 760 [mmHg], the values of $DO_{\text{sat}}(T(t))$ were derived. The dependence between $DO_{\text{sat}}(T(t))$ and temperature variation is shown in Fig. 1. The values presented in Fig. 1 were then used to build the time trajectory $DO_{\text{sat}}(T(t))$ representing a repeating summer day. This trajectory is illustrated in Fig. 2.

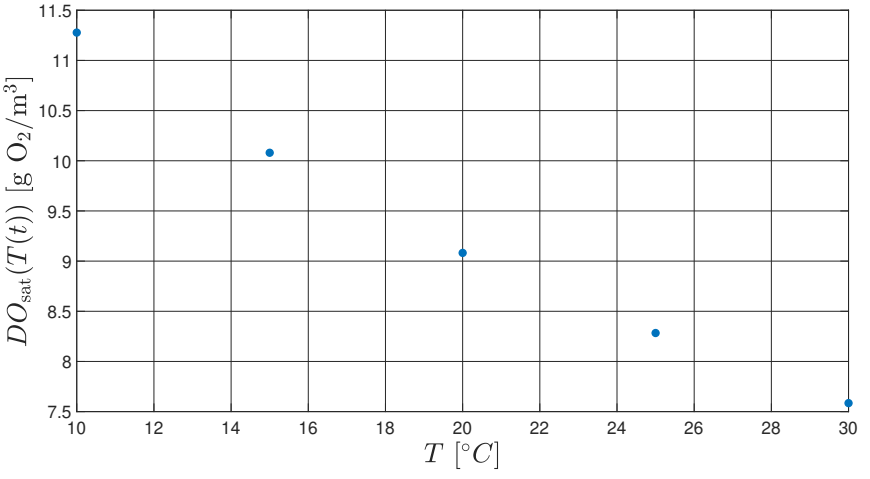

Figure 1: The dependence between $DO_{\text{sat}}(T(t))$ and temperature.

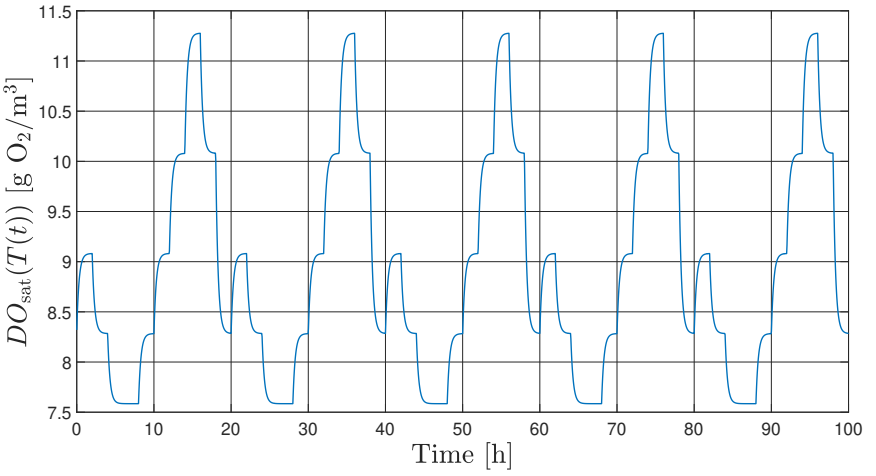

Figure 2: The trajectory of $DO_{\text{sat}}(T(t))$.

The range of values for the bioreactor airflow trajectory $Q_{\text{air}}(t)$, i.e., 1500 - 3000 $\left[\text{m}^3/\text{h}\right]$, was derived from the range of this variable in the Swarzewo SBR WWTP, which is directly related to the power of the blowers installed in the aeration system of this WWTP [37]. However, the variability (shape) of this trajectory within this range was established based on other trajectories of this variable available in the literature. The trajectory obtained in this way is shown in Fig. 3.

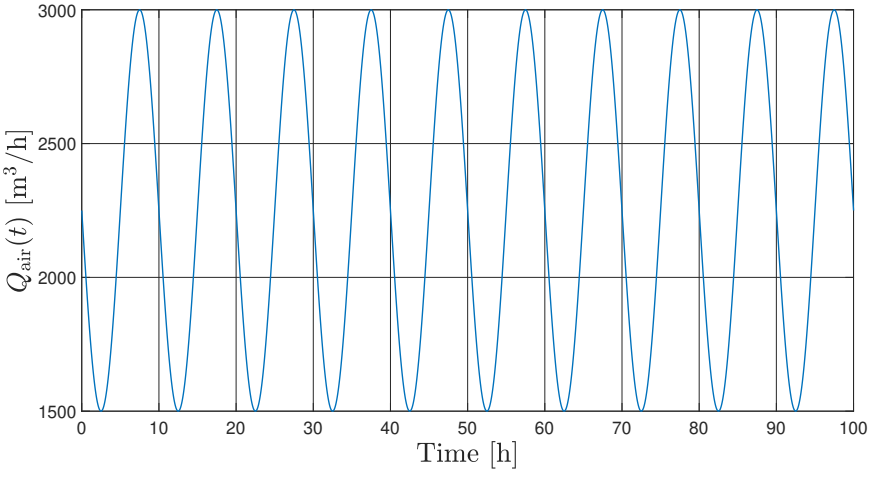

Figure 3: The trajectory of airflow $Q_{\text{air}}(t)$.

Similarly, the range of values of the respiration trajectory $R(t)$ shown in Fig. 4 was derived from the range of this variable in the Swarzewo SBR WWTP during its typical operation in the aerobic phase. This range is 2.8 - 4.03 $\left[\text{g}/\text{m}^3\ \text{h}\right]$. In turn, the variability of this trajectory was assumed on the basis of other trajectories of this variable available in the literature.

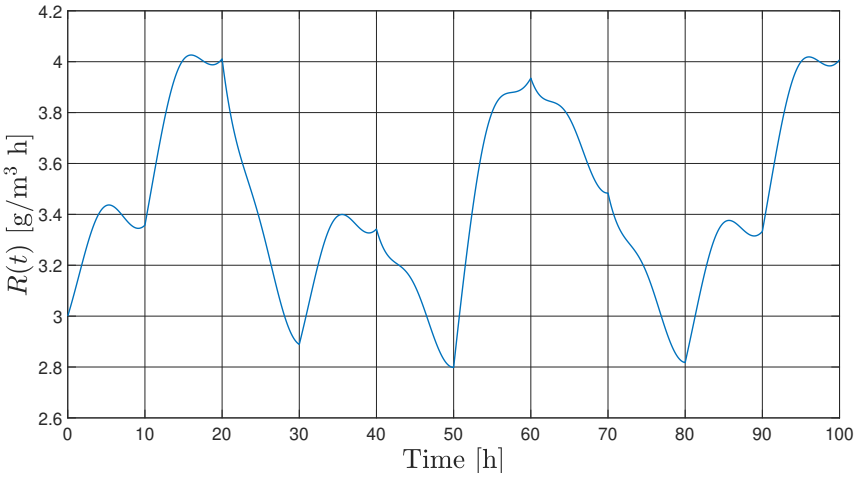

Figure 4: The trajectory of respiration $R(t)$.

Next, using the prepared $DO_{\text{sat}}(T(t))$, $Q_{\text{air}}(t)$, and $R(t)$, and taking into account Assumption 1, where $k_{\text{L}}a\left(Q_{\text{air}}(t)\right) = \alpha Q_{\text{air}}(t)$ with the value of parameter α assumed from the SIMBA simulator [19], i.e., $\alpha = 0.208$ [1/m^3], and also assuming the value of parameter $K_{\text{DO}}(t) = 0.2$ [g O_2/m^3], model (1) was solved and thus the trajectory $DO(t)$ was obtained. It should be added that the obtained range of values of the $DO(t)$ trajectory (see Fig. 7), i.e. 0.5 - 5 $\left[\text{g } O_2/\text{m}^3\right]$ is consistent with the range of $DO(t)$ measurements in the Swarzewo SBR WWTP under the considered conditions. Finally, multiplying the trajectory $R(t)$ and the Monod-type term (with the assumed $K_{\text{DO}}(t)$ and the obtained $DO(t)$ trajectory), the trajectory of respiration rate $\tilde{R}(t)$ was obtained. This trajectory is shown in Fig. 5.

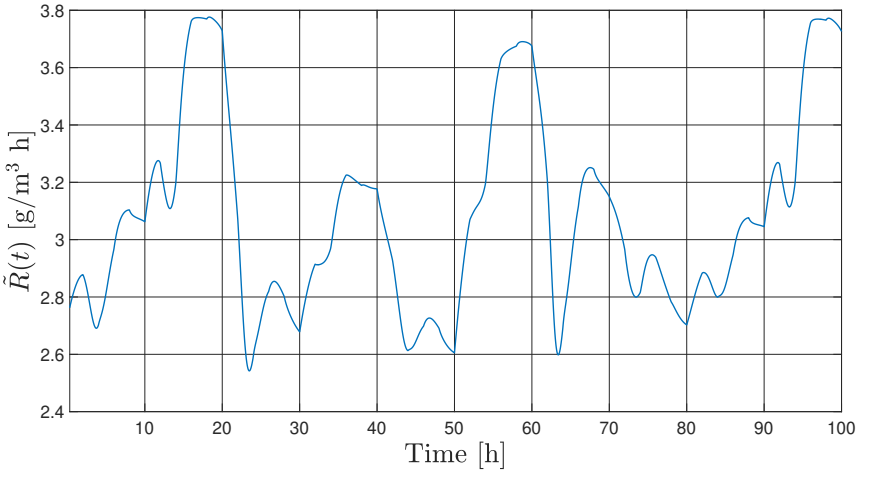

Figure 5: The trajectory of respiration rate $\tilde{R}(t)$.

According to Assumption 3, the measurably available state variable is the dissolved oxygen concentration. Typically, $DO(t)$ is measured by measuring devices which are characterised by negligible measurement error, the presence of measurement noise, and certain dynamics which can be approximated by first-order inertia with a time constant of about 40 - 60 [sec] [24]. Therefore, it was assumed that the measurement error can be neglected, and also the measurements are burdened with measurement noise modelled as white Gaussian noise with standard deviation equal to 0.03 $\left[\text{g } O_2/\text{m}^3\right]$ [4, 41], whereas the dynamics of the measuring device are modelled as first-order inertia with the time constant $T_{\text{sensor}} = 1/60$ [h]. Moreover, according to the datasheets of typical dissolved oxygen concentration sensors, the available measurement range is between 0.0 and 20.0 $\left[\text{g } O_2/\text{m}^3\right]$, and the resolution-related measurement quantisation interval is 0.01 $\left[\text{g } O_2/\text{m}^3\right]$. To match up the introduced features of the measuring device, the model shown in Fig. 6 was implemented in the Matlab/Simulink environment.

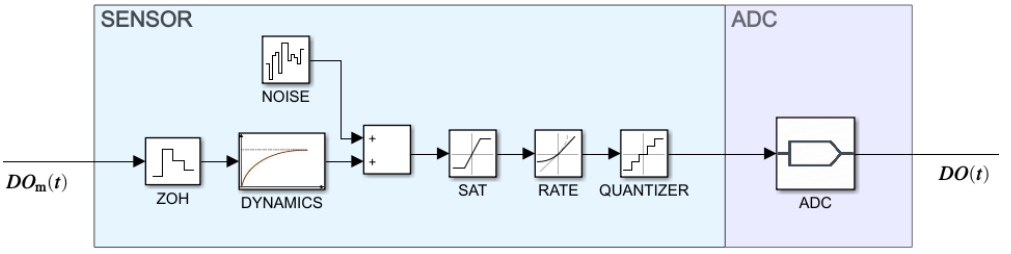

Figure 6: The diagram of the measuring device model.

The 'NOISE' and 'DYNAMICS' blocks in Fig. 6 represent the measurement noise, and the dynamics of the measuring device, respectively. In turn, the input sampling, measurement saturation level, rate of change of the signal and output value quantisation are realised by 'ZOH', 'SAT', 'RATE' and 'QUANTISER' blocks, respectively. The rate limiter-related parameter's value was set to $\mathcal{R}_{\mathrm{s}} = \pm 100$ [−] whereas the sensor related sample time was selected as $T_{\mathrm{ss}} = 3/3600$ [h]. The dissolved oxygen concentration measurement is performed by utilising classical $4 - 20$ [mA] current loop, which analogue signal is subsequently converted to its digital equivalent. Hence, the simple model of a 16-bit analog-to-digital converter ('ADC' block in Fig. 6) was proposed. The 'ADC' consists of the *min-max* procedure conversion blocks for transforming analogue and digital values of particular signals, sampling component, and quantisation block. Thus, for the converter modelling purposes, the sample time was selected as $T_{\mathrm{s}} = 1/3600$ [h] whereas the quantisation interval is $\mathcal{Q}_{\mathrm{ADC}} = (20 - 4)/(2^{16}) = 0.000244$ [−]. $DO(t)$ measurement results obtained from the measuring device modelled in this way were filtered by the proposed low-pass filter filtered measurement results obtained from the measuring device with the time constant $T_{\mathrm{F}} = 3/60$ [h]. The obtained dissolved oxygen concentration trajectories: real (blue line - $DO_{\mathrm{m}}(t)$), measured (orange line), and filtered (yellow line) are shown in Fig. 7. For clarity, Fig. 8 shows a zoomed-in fragment of the trajectories from Fig. 7.

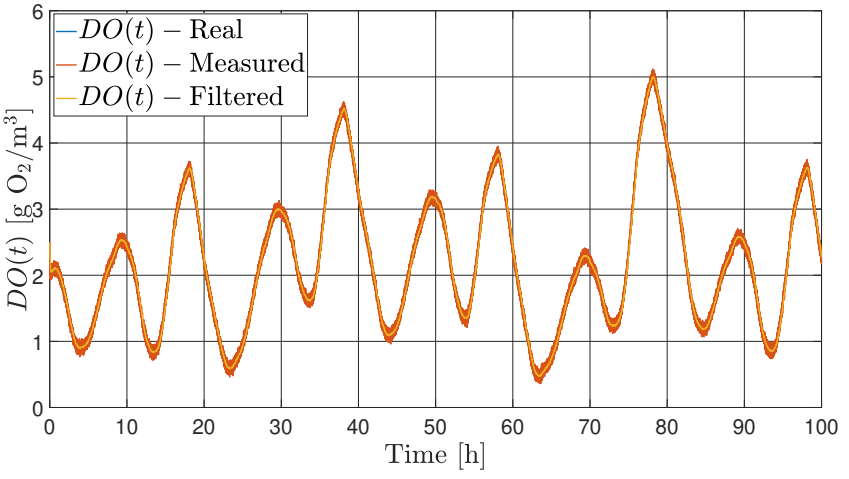

Figure 7: Trajectories of the dissolved oxygen concentration $DO(t)$.

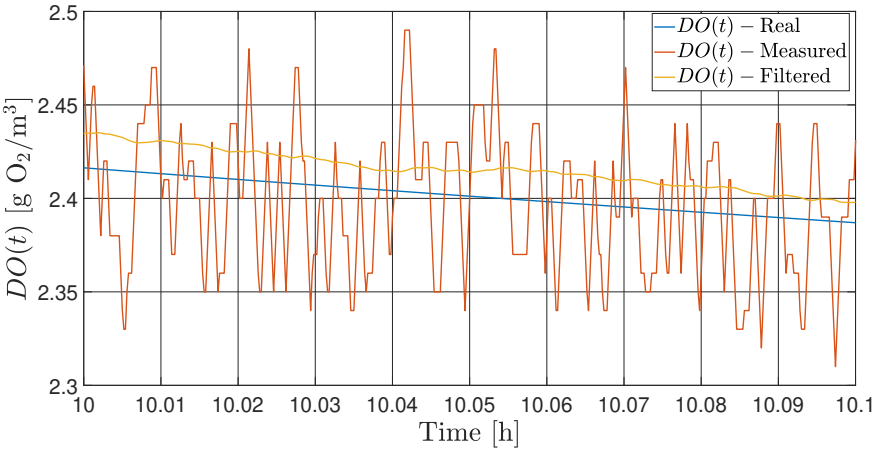

Figure 8: A zoomed-in fragment of the dissolved oxygen concentration trajectories.

Taking these considerations into account, a series of simulation experiments have been carried out, the selected results of which are presented in the following sections.

4.1. Estimation results – noise free scenario

In this scenario, the impact of measurement device dynamics and measurement noise is neglected to show the estimation performance without any particular disturbances. For the assumed initial conditions of the state variables, i.e., $\boldsymbol{x}_0 = \begin{bmatrix}2 & 2.73\end{bmatrix}^{\mathrm{T}}$, and initial conditions of their estimates, i.e., $\hat{\boldsymbol{x}}_0 = \begin{bmatrix}2.5 & 0\end{bmatrix}^{\mathrm{T}}$, the reconstruction performance of ALO and STSMO has been examined. The observers gains selected according to the methodology presented in Sections 3.1 and 3.2 were as follows: $\zeta = 0.7$, $\omega = 50$ for ALO; $\beta_1 = 15$, $\beta_2 = 15$, $\bar{r} = 10$, $\gamma = 0.01$, $c = 1000$ for STSMO. The trajectories of state variables representing $DO(t)$ and $\tilde{R}(t)$ (see (2) and (3)) which were generated by model (1) (see also Section 4) and their estimates from ALO (13) and STSMO (20) are shown in Figs. 9 and 10, respectively. It is worth emphasising that the time scale was assumed to 100 hours, what was related to the biological properties of the process, whereas the simulation step was selected as T_{s}.

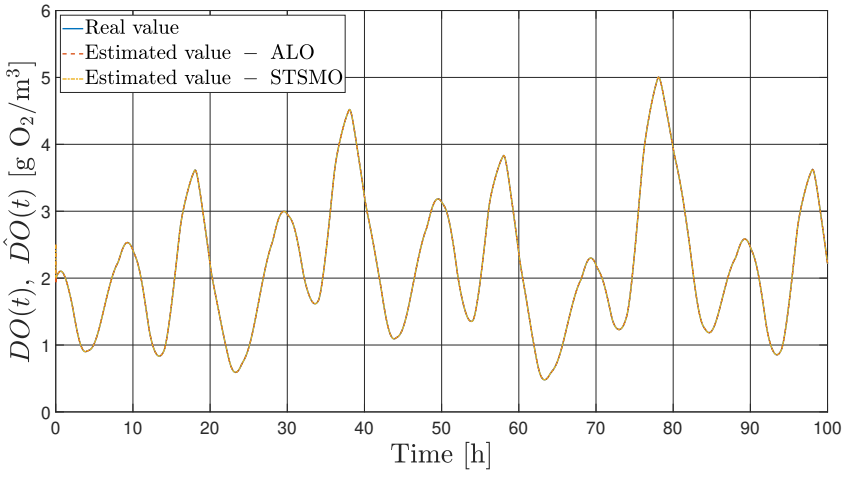

Figure 9: Trajectories of $DO(t)$ and its estimates $\hat{DO}(t)$ generated by ALO and STSMO - noise free scenario.

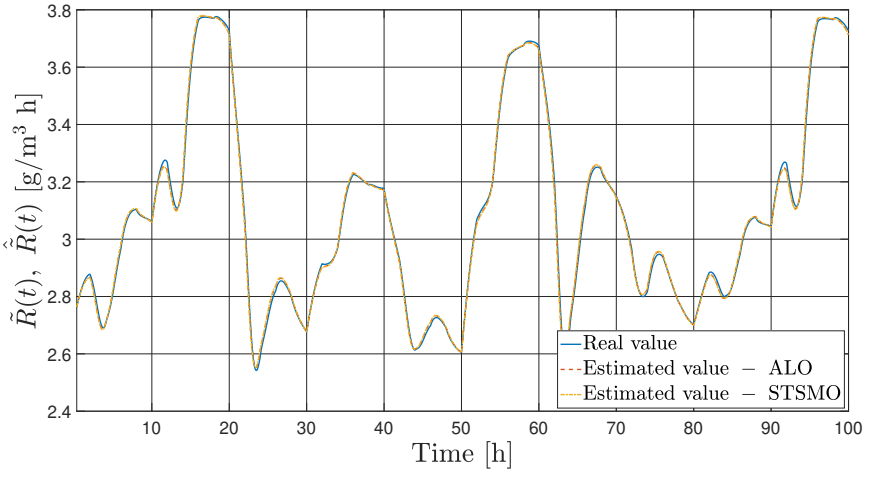

Figure 10: Trajectories of $\tilde{R}(t)$ and its estimates $\hat{\tilde{R}}(t)$ generated by ALO and STSMO - noise free scenario.

When analysing the trajectories shown in Fig. 9 it can be deduced that the dissolved oxygen concentration, which is measurably available, is reconstructed with practically zero estimation error by both of the developed observers. This estimation performance for this state variable occurred in all experiments. Therefore, further experiments will be illustrated only by invoking to the results obtained for the respiration rate. As can be seen in Fig. 10, the trajectories of the generated estimates are very close to the trajectory of the reconstructed (unmeasured) variable. The small estimation error is mainly caused by the stability and boundedness aspects, discussed in detail in Sections 3.1 and 3.2. To precisely depict the accuracy of both observers, Fig. 11 presents the relative percentage estimation error $e_2^{\text{rel}}(t) \in \mathbb{R}$ for the respiration rate reconstruction.

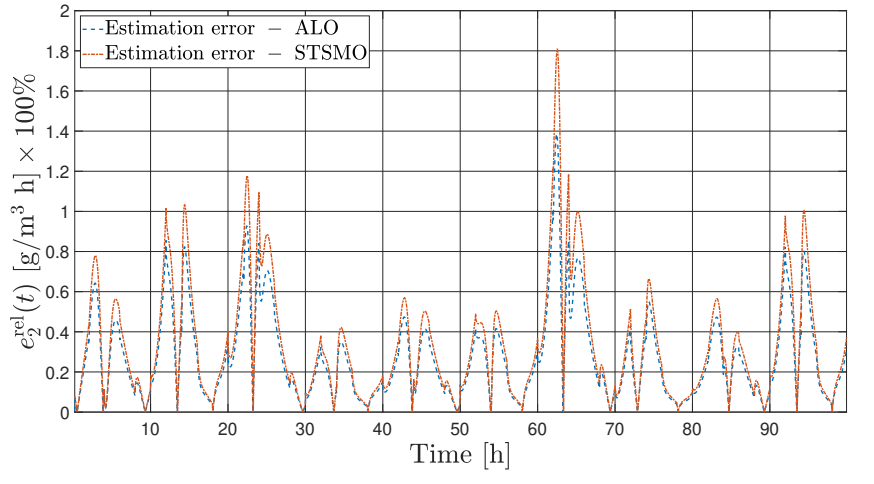

Figure 11: Relative percentage estimation error for respiration rate - noise free scenario.

As can be noticed in Fig. 11, the relative percentage estimation error for ALO and STSMO does not exceed 2%. Even though the obtained estimation performance is high, it is not the same for both observers. It results directly from the way how the estimate is generated by the given algorithm. For ALO, the global uniform boundedness is guaranteed by definition; however, as it has been emphasised in Remark 2, an appropriate selection of ζ and ω provides a narrow size of the estimation error boundary in the steady state. In turn, for STSMO, exact convergence is not given because of the utilisation of the approximation functions (22) and (23) to compensate the impact of the chattering phenomenon (see Remarks 3 and 4). Even if β_1 and β_2 are well selected and $\overline{r}$ 'catches' the variation of $r(t)$, the introduced modifications 'break' the global uniform stability of the estimation error.

4.2. Estimation results – noise affected scenario

In this scenario, the impact of the measurement device dynamics and the measurement noise has been included to show the estimation performance when the dissolved oxygen concentration measuring process is disturbed. The properties of the measuring device model and the measurement noise parameters were directly incorporated from Section 4. The entire study was conducted in the same way as in Section 4.1; hence, the initial conditions of state variables and their estimates were the same as in the previous research. Also, the observer's gains were selected in the same way; however, due to the measurement noise occurrence, they are as follows: $\zeta = 0.8$, $\omega = 30$ for ALO; $\beta_1 = 10$, $\beta_2 = 10$, $\bar{r} = 10$, $\gamma = 0.1$, $c = 100$ for STSMO. The trajectories of the state variable representing $\tilde{R}(t)$ and their estimates from ALO (13) and STSMO (20) are shown in Fig. 12.

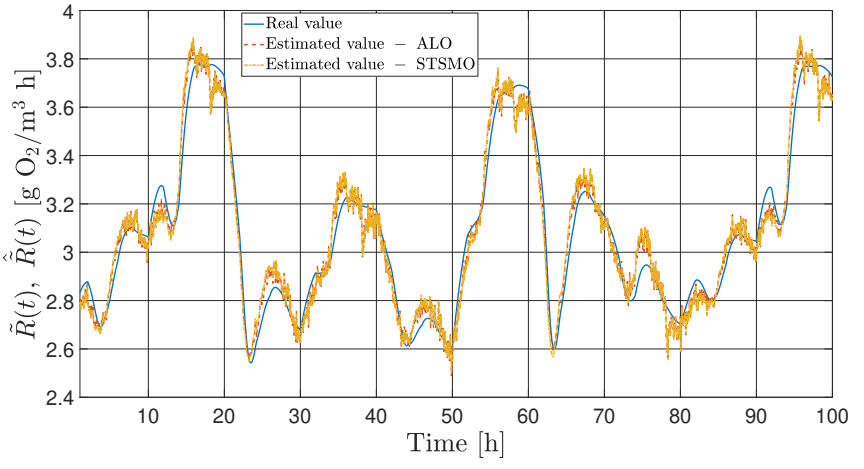

Figure 12: Trajectories of $\tilde{R}(t)$ and its estimates $\hat{\tilde{R}}(t)$ generated by ALO and STSMO - noise affected scenario.

As can be seen in Fig. 12, the trajectories of the generated estimates deviate from the trajectory of the reconstructed (unmeasured) variable. The boundedness of the estimation error is preserved; however, the estimation performance is lower compared to the results shown in Fig. 10. To precisely depict the obtained estimation performance, Fig. 13 shows the relative percentage estimation error $e_2^{\text{rel}}(t) \in \mathbb{R}$ for respiration rate reconstruction.

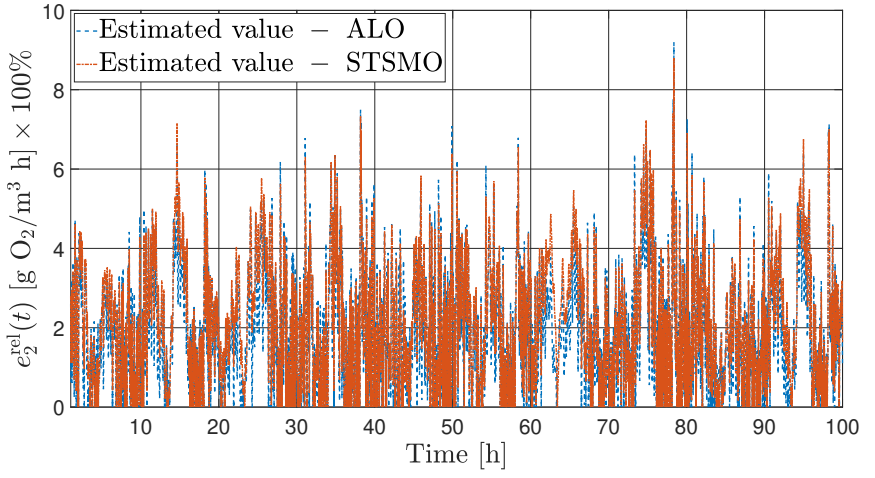

Figure 13: Relative percentage estimation error for respiration rate - noise affected scenario.

As can be noticed in Fig. 13, the relative percentage estimation error for ALO and STSMO occasionally exceeds 7%. Like in the experiment described in Section 4.1, the estimation performance differs for the developed observers, although the difference is slight. The reasons for this are analogous to those indicated in Section 4.1. Naturally, a

higher value of the estimation error is due to the measurement conditions of $DO(t)$. However, the resulting estimation performance is still high enough for the obtained results to be considered satisfactory.

5. Conclusions

In this paper, the problem of respiration rate estimation using two new non-linear observers for wastewater treatment plants has been investigated. In particular, the non-linear adaptive Luenberger-like observer and the super-twisting sliding mode observer were devised to produce stable and bounded estimates of the respiration rate. The global uniform boundedness of the produced estimates or the global uniform asymptotic stability of the estimation error were rigorously proved using the Lyapunov stability theory. For the observers' synthesis purposes, the correct utility model was derived and its observability was demonstrated. The designed observers were applied to the non-linear model of dissolved oxygen concentration dynamics. The entire system was implemented in the Matlab/Simulink environment. The performance of the developed observers was validated by simulation using data whose ranges correspond to the data from the Swarzewo SBR WWTP. The satisfactory performance of the generated estimates was obtained, which confirms the high effectiveness of the devised observers. The estimation performance is comparable, although it is possible to identify some features of the developed observers that distinguish them from each other. The most important features of the non-linear adaptive Luenberger-like observer are as follows:

- the observer guarantees a global boundedness of the estimation error to a certain sphere related to the error norm;
- a simple selection of observer gains based on the allocation of the linear second-order system eigenvalues;
- if measurement noise is present, there is a need to filter it;
- the observer has good dynamic properties;
- a simple software implementation of the algorithm.

In turn, the most important features of the super twisting sliding mode observer yield:

- the observer guarantees global asymptotic stability of the estimation error (also with fixed time - uniformly);
- selection of observer gains from the numerically determined admissible region (established for any case of the algorithm application);
- the need to approximate the $|\cdot|$ and $\mathrm{sgn}(\cdot)$ functions occurring in the observer structure with continuous equivalents;
- if measurement noise is present, there is a need to filter it;
- the observer has very good dynamic properties;
- the software implementation of the algorithm is not complicated but requires skillful introduction of approximating functions and their tuning.

The trajectories of the generated respiration rate estimates can be applied both in the monitoring system of the state of ongoing processes in the wastewater treatment plant and in the dissolved oxygen control systems. This is due to the fact that respiration is the main indicator of current sewage load and biomass activity, while its measurements are not common in wastewater treatment plants.

References

[1] Baird, R., Eaton, A., Rice, E., 2017. Standard Methods for the examination of water and wastewater, 23rd Edition. American Public Health Association, Washington, DC, US.

[2] Bastin, G., Dochain, D., 1986. On-line estimation of microbial specific growth rates. Automatica 22, 705–709. doi:https://doi.org/10.1016/0005-1098(86)90007-5.

[3] Bastin, G., Dochain, D., 1990. On-line estimation and adaptive control of bioreactors. Elsevier, Amsterdam, Netherlands.

[4] Carlsson, B., Wigren, T., 1993. On-line identification of the dissolved oxygen dynamics in an activated sludge process. IFAC Proceedings Volumes 26, 215–220. doi:https://doi.org/10.1016/S1474-6670(17)48717-9.

[5] Claes, J.E., Ryckaert, V.G., Gerards, R., Vriens, L., Van Impe, J.F., 1997. Modeling, monitoring and control of cyclically operated biological wastewater treatment plants, in: 1997 European Control Conference (ECC), pp. 2623–2628. doi:10.23919/ECC.1997.7082503.

[6] Czyżniewski, M., Łangowski, R., 2022. A robust sliding mode observer for non-linear uncertain biochemical systems. ISA T. 123, 25–45. doi:https://doi.org/10.1016/j.isatra.2021.05.040.

[7] Czyżniewski, M., Łangowski, R., 2023. An analysis of observability and detectability for different sets of measured outputs - CSTR case study, in: Kowalczuk, Z. (Ed.), Intelligent and Safe Computer Systems in Control and Diagnostics, Springer International Publishing, Cham. pp. 352–363.

[8] De Battista, H., Picó, J., Garelli, F., Navarro, J.L., 2012. Reaction rate reconstruction from biomass concentration measurement in bioreactors using modified second-order sliding mode algorithms. Bioproc. Biosyst. Eng. 35, 1615–1625. doi:10.1007/s00449-012-0752-y.

[9] De Battista, H., Picó, J., Garelli, F., Vignoni, A., 2011. Specific growth rate estimation in (fed-)batch bioreactors using second-order sliding observers. J. Process Control 21, 1049–1055. doi:https://doi.org/10.1016/j.jprocont.2011.05.008.

[10] Distefano, J., 2015. Dynamic systems biology modeling and simulation. Academic Press, Cambridge, MA, US.

[11] Dochain, D., Bastin, G., 1985. Stable adaptive algorithms for estimation and control of fermentation processes. IFAC Proceedings Volumes 18, 37–42. doi:https://doi.org/10.1016/S1474-6670(17)59890-0.

[12] Dochain, D., Vanrolleghem, P., 2001. Dynamical modelling and estimation in wastewater treatment processes. IWA Publishing, London, UK.

[13] Fairman, F., 1998. Linear control theory: the state space approach. John Wiley & Sons, Springdale, AR, US.

[14] Fridman, L., Moreno, J.A., Iriarte, R., 2011. Sliding modes after the first decade of the 21st century. Springer-Verlag, Berlin, Germany.

[15] Gerkšič, S., Vrečko, D., Hvala, N., 2006. Improving oxygen concentration control in activated sludge process with estimation of respiration and scheduling control. Water Sci. Technol. 53, 283–291. doi:https://doi.org/10.2166/wst.2006.133.

[16] Henze, M., Gujer, W., Mino, T., Van Loosdrecht, M., 2000. Activated sludge models ASM1, ASM2, ASM2d and ASM3. IWA Publishing, London, UK.

[17] Horan, N.J., 1990. Biological wastewater treatment systems - theory and operation. John Wiley & Sons, Chichester, UK.

[18] Hvala, N., Bavdaz, G., Kocijan, J., 2001. Nonlinear state and parameter estimation in batch biological wastewater treatment. Int. J. Syst. Sci. 32, 145–156. doi:10.1080/00207720117693.

[19] IFAK Technology, . Simba. user's Guide. https://www.ifak.eu/en/produkte/simba. Accessed: 2022-10-04.

[20] Jeppsson, U., Olsson, G., 1993. Reduced order models for on-line parameter identification of the activated sludge process. Water Sci. Technol. 28, 173–183. doi:10.2166/wst.1993.0657.

[21] Khalil, H.K., 2002. Nonlinear systems. 3 ed., Prentice-Hall, Inc., Upper Saddle River, NJ, US.

[22] Łangowski, R., Brdys, M.A., 2018. An optimised placement of the hard quality sensors for a robust monitoring of the chlorine concentration in drinking water distribution systems. J. Process Control 68, 52–63. doi:https://doi.org/10.1016/j.jprocont.2018.04.007.

[23] Levant, A., 2003. Higher-order sliding modes, differentiation and output-feedback control. Int. J. Control 76, 924–941. doi:10.1080/0020717031000099029.

[24] Lindberg, C.F., 1997. Control and estimation strategies applied to the activated sludge process. Ph.D. thesis. Uppsala University. Uppsala, Sweden.

[25] Lindberg, C.F., Carlsson, B., 1996. Estimation of the respiration rate and oxygen transfer function utilizing a slow do sensor. Water Sci. Technol. 33, 325–333. doi:https://doi.org/10.1016/0273-1223(96)00185-0.

[26] Lukasse, L.J.S., Keesman, K.J., Van Straten, G., 1997. Estimation of BODst, respiration rate and kinetics of activated sludge. Water Res. 31, 2278–2286. doi:https://doi.org/10.1016/S0043-1354(97)00047-X.

[27] Marsili-Libelli, S., Tabani, F.T., 2002. Accuracy analysis of a respirometer for activated sludge dynamic modelling. Water Res. 36, 1181–1192. doi:10.1016/s0043-1354(01)00339-6.

[28] Moreno, J.A., Dochain, D., 2008. Global observability and detectability analysis of uncertain reaction systems and observer design. Int. J. Control 81, 1062–1070. doi:10.1080/00207170701636534.

[29] Moreno, J.A., Osorio, M., 2012. Strict Lyapunov functions for the super-twisting algorithm. IEEE T. Automat. Contr. 57, 1035–1040. doi:10.1109/TAC.2012.2186179.

[30] Moreno, J.A., Rocha-Cózatl, E., Vande Wouwer, A., 2014. A dynamical interpretation of strong observability and detectability concepts for nonlinear systems with unknown inputs: application to biochemical processes. Bioproc. Biosyst. Eng. 37, 37–49. doi:10.1007/s00449-013-0915-5.

[31] Nuñez, S., De Battista, H., Garelli, F., Vignoni, A., Picó, J., 2013. Second-order sliding mode observer for multiple kinetic rates estimation in bioprocesses. Control Eng. Pract. 21, 1259–1265. doi:https://doi.org/10.1016/j.conengprac.2013.03.003.

[32] Olsson, G., Newell, B., 1999. Wastewater treatment systems. Modelling, diagnosis and control. IWA Publishing, London, UK.

[33] Perrier, M., de Azevedo, S.F., Ferreira, E.C., Dochain, D., 2000. Tuning of observer-based estimators: theory and application to the on-line estimation of kinetic parameters. Control Eng. Pract. 8, 377–388. doi:https://doi.org/10.1016/S0967-0661(99)00164-1.

[34] Petersen, B., 2000. Calibration, identifiability and optimal experimental design of activated sludge model. Ph.D. thesis. University of Gent. Gent, Belgium.

[35] Picó, J., De Battista, H., Garelli, F., 2009. Smooth sliding-mode observers for specific growth rate and substrate from biomass measurement. J. Process Control 19, 1314–1323. doi:https://doi.org/10.1016/j.jprocont.2009.04.001.

[36] Piotrowski, R., Brdys, M.A., Konarczak, K., Duzinkiewicz, K., Chotkowski, W., 2008. Hierarchical dissolved oxygen control for activated sludge processes. Control Eng. Pract. 16, 114–131. doi:https://doi.org/10.1016/j.conengprac.2007.04.005.

[37] Piotrowski, R., Skiba, A., 2015. Nonlinear fuzzy control system for dissolved oxygen with aeration system in sequencing batch reactor. Inf. Technol. Control 44, 182–195. doi:https://doi.org/10.5755/j01.itc.44.2.7784.

[38] Schaum, A., Moreno, J.A., Vargas, A., 2005. Global observability and detectability analysis for a class of nonlinear models of biological processes with bad inputs, in: 2005 2nd International Conference on Electrical and Electronics Engineering, pp. –. doi:10.1109/ICEEE.2005.1529640.

[39] Schmidt, M., Fung, G., 2007. Fast optimization methods for L1 regularization: A comparative study and two new approaches, in: Kok, J.N., Koronacki, J., Mantaras, R.L.D., Matwin, S., Mladenič, D., Skowron, A. (Eds.), Machine Learning: ECML 2007. ECML 2007. Lecture Notes in Computer Science, Springer International Publishing, Berlin, Heidelberg. pp. 286–297.

[40] Silva, F. J. S. de Macêdo, E.C.T., Catunda, S.Y.C., Dorea, C.E.T., van Haandel, A.C., 2016. Disturbance observer for estimation of oxygen uptake rate in an activated sludge reactor, in: 2016 IEEE International Instrumentation and Measurement Technology Conference Proceedings, pp. 1–6. doi:10.1109/I2MTC.2016.7520516.

[41] Silva, F.J.S., Catunda, S.Y.C., Neto, J.V.F., van Haandel, A.C., 2010. Dissolved oxygen PWM control and oxygen uptake rate estimation using Kalman filter in activated sludge systems, in: 2010 IEEE Instrumentation & Measurement Technology Conference Proceedings, pp. 579–584. doi:10.1109/IMTC.2010.5488094.

[42] Spanjers, H., Vanrolleghem, P., Olsson, G., Doldt, P., 1996. Respirometry in control of the activated sludge process. Water Sci. Technol. 34, 117–126. doi:https://doi.org/10.1016/0273-1223(96)84211-9.

[43] Suchodolski, T., Brdys, M.A., Piotrowski, R., 2007. Respiration rate estimation for model predictive control of dissolved oxygen in wastewater treatment plant. IFAC Proceedings Volumes 40, 286–291. doi:https://doi.org/10.3182/20070723-3-PL-2917.00046.

[44] Utkin, V., 1992. Sliding modes in control and optimizations. Springer-Verlag, Berlin, Germany.

[45] Villaverde, A.F., 2019. Observability and structural identifiability of nonlinear biological systems. Complexity 2019, 8497093, 13. doi:https://doi.org/10.1155/2019/8497093.

[46] Yoo, C.K., Lee, I.B., 2004. Soft sensor and adaptive model-based dissolved oxygen control for biological wastewater treatment processes. Environ. Eng. Sci. 21, 331–340. doi:https://doi.org/10.1089/109287504323066978.

[47] Young, J., Cowan, R., 2004. Respirometry for environmental science and engineering. SJ Enterprises, Springdale, AR, US.

[48] Zubowicz, T., 2018. Decentralized tracking of dissolved oxygen concentration in interacting multi zone bioreactor by supervised PI controller. Ph.D. thesis. Gdańsk University of Technology. Gdańsk, Poland.

Mateusz Czyżniewski received the M.Sc. degree (Hons.) in control engineering from the Faculty of Electrical and Control Engineering at the Gdańsk University of Technology in 2019. Since October 2019, he has been a Ph.D. student at the Gdańsk University of Technology in the field of Control Engineering. His research interests involve advanced non-linear control theory, numerical simulation, design of computer control systems, mathematical modelling of dynamical systems, and robust estimation and monitoring methods.

Rafał Łangowski received the M.Sc. and the Ph.D. degrees (Hons.) in control engineering from the Faculty of Electrical and Control Engineering at the Gdańsk University of Technology in 2003 and 2015, respectively. From 2007 to 2014, he held the specialist as well as manager positions at ENERGA, one of the biggest energy enterprises in Poland. He is currently an Assistant Professor with the Department of Intelligent Control and Decision Support Systems at the Gdańsk University of Technology. His research interests involve mathematical modelling and identification, estimation methods, especially state observers, and monitoring of large-scale complex systems.

Robert Piotrowski received the M.Sc. Ph.D. and D.Sc. degrees (Hons.) in control engineering from the Faculty of Electrical and Control Engineering at the Gdańsk University of Technology in 2001, 2005 and 2018, respectively. He is currently an Associate Professor with the Department of Intelligent Control and Decision Support Systems. His research interests involve mathematical modelling, control design of non-linear dynamical systems, and design of computer control systems.